

Oxygen and Carbon Isotope Composition in Primary Carbonatites of the World: Data Summary and Linear Trends

Alexander V. Bolonin

Central Geological Research Institute for Nonferrous and Precious Metals (TSNIGRI), Moscow, Russia

Email: bolonin.a@inbox.ru

How to cite this paper: Bolonin, A.V. (2019) Oxygen and Carbon Isotope Composition in Primary Carbonatites of the World: Data Summary and Linear Trends. *Open Journal of Geology*, **9**, 424-439.
<https://doi.org/10.4236/oig.2019.98028>

Received: July 10, 2019

Accepted: August 20, 2019

Published: August 23, 2019

Copyright © 2019 by author(s) and Scientific Research Publishing Inc. This work is licensed under the Creative Commons Attribution International License (CC BY 4.0).
<http://creativecommons.org/licenses/by/4.0/>



Open Access

Abstract

The article contains the results of statistical processing of a large summary of $\delta^{18}\text{O}$ - $\delta^{13}\text{C}$ isotope values in the primary carbonatites of the world. From literary sources, 1593 paired values $\delta^{18}\text{O}$ - $\delta^{13}\text{C}$ from 173 carbonatite occurrences of the world were collected. This report exceeds all previously published reports on C-O isotopes in carbonatites by quantity of the used values and carbonatite occurrences. Statistical data analysis is performed on diagrams in the coordinates $\delta^{18}\text{O}$ (‰, V-SMOW) - $\delta^{13}\text{C}$ (‰, V-PDV). For each carbonatite occurrence, not only the arithmetic mean values are calculated, but also the regression line. Distinct linear trend of $\delta^{18}\text{O}$ - $\delta^{13}\text{C}$ values is found in half of the carbonatite occurrences. The starting, middle, and ending points of the trend line are determined. The slope of the trend line (angular coefficient) varies over a wide range. The trend is dominated by an average angular coefficient of 0.30 (positive correlation $\delta^{18}\text{O}$ - $\delta^{13}\text{C}$). In the literature, it is associated with the Rayleigh high-temperature fractionation of carbonatite melts or with their sedimentary contamination. Half of the carbonatite occurrences do not show a linear trend of $\delta^{18}\text{O}$ - $\delta^{13}\text{C}$ values, probably due to the combined action of multidirectional trends. The initial ratio $^{87}\text{Sr}/^{86}\text{Sr}$ in the used carbonatite occurrences varies from 0.701 to 0.708. Statistics show no correlation of $^{87}\text{Sr}/^{86}\text{Sr}$ with the $\delta^{18}\text{O}$ - $\delta^{13}\text{C}$ system.

Keywords

Carbonatite Occurrences, Oxygen, Carbon and Strontium Isotopes, Linear Trends

1. Introduction

Oxygen and carbon isotope composition of carbonatites were summarized in a

number of previous works. The largest number of $\delta^{18}\text{O}$ - $\delta^{13}\text{C}$ values (about 440) was collected and used to construct histograms in [1]. In the work [2], 56 values from 8 carbonatite occurrences of Kola Alkaline Province were used, linear trends were identified. In the work [3], 70 analyzes from 20 carbonatite occurrences of Siberia and Mongolia were used; a diagram was proposed for determining the type of mantle using the ratio of O-C isotopes. In the work [4], the fields of point values are outlined in the $\delta^{18}\text{O}$ - $\delta^{13}\text{C}$ diagram for the Greenland, Europe, and North and South America regions without a division for individual carbonatite occurrences. The fields of primary igneous carbonatites on the $\delta^{18}\text{O}$ - $\delta^{13}\text{C}$ diagram are outlined in the works [1] [5] [6] [7]. These fields are used in the analysis of local isotope data in carbonatite studies.

This paper uses 1593 pairs of conjugate values of $\delta^{18}\text{O}$ - $\delta^{13}\text{C}$ out of 173 carbonatite occurrences of the world. In addition, a linear regression analysis of the values is performed for most occurrences. This paper exceeds all previously published reports on C-O isotopes in carbonatites by quantity of the used values and carbonatite occurrences. Data on the ratio $^{87}\text{Sr}/^{86}\text{Sr}$ in 92 carbonatite occurrences are taken additionally from the sources used. The limited size of the article does not allow to provide a complete database and a list of used references (about 100 titles).

Carbonatite occurrences are represented by bodies of various shapes and sizes (complexes, massifs, dikes, facies zones). Isotope analysis is applied to carbonatite rocks (sovite, alvikite, beforsite, etc.), monofractions of calcite, dolomite, ankerite, siderite. Authors of literature classify the analyzed material as primary carbonatites (PC). This is mainly done on the basis of petrographic studies, in which secondary endo- and exogenous minerals are not detected. Single anomalous values are excluded from the primary category by the author of the article. Numerous $\delta^{18}\text{O}$ - $\delta^{13}\text{C}$ values refer to secondary carbonatites in the used literature: carbonate tuffs and lavas, hydrothermal veins, hydrothermally altered and recrystallized carbonatites, weathered and oxidized carbonatites, secondary calcite. Data on secondary carbonatites is not used in this article.

All isotope diagrams have a horizontal x -axis $\delta^{18}\text{O}$ (‰, V-SMOW) and a vertical y -axis $\delta^{13}\text{C}$ (‰, V-PDV). The equal scale of both axes, a multiple of 1‰, allows to visually comparing the shape of the point sets (point fields) and the slope of the trend lines. The names of carbonatite occurrences and their identification number (ID) are coordinated with the database [8] and are given in English transcription.

2. Summary Data

The diagram in **Figure 1** contains 1593 points of the $\delta^{18}\text{O}$ - $\delta^{13}\text{C}$ from 173 carbonatite occurrences, including various carbonatite facies in one occurrence. The number of points in the individual occurrences varies from 2 to 54. The points fill a very wide field. Analysis of the field is complex and incorrect due to the variable number and large scatter of points that characterize individual carbonatite occurrences. The contours PC-98% and PC-90% presented in the diagram are proved in **Figure 2** and **Figure 3**.

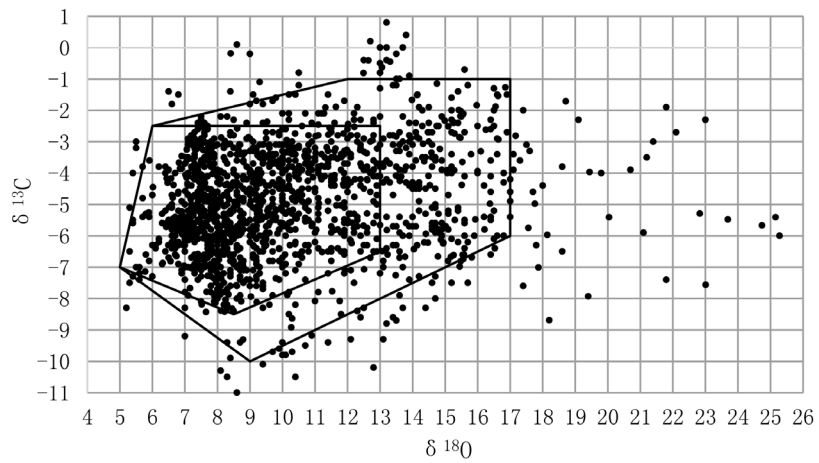


Figure 1. Primary carbonatites (PC) of the world: a summary of $\delta^{18}\text{O}$ - $\delta^{13}\text{C}$ paired values ($n = 1593$) and contours PC-98% (external) and PC-90% (internal).

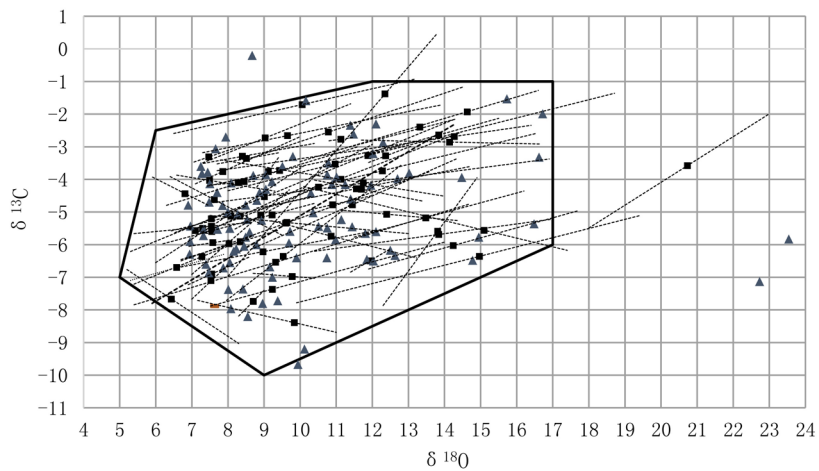


Figure 2. Trend lines and middle points (black square) in occurrences with a linear trend ($n = 70$). Only middle points (black triangle) in other occurrences ($n = 103$). Polygonal contour PC-98% includes 98% of points.

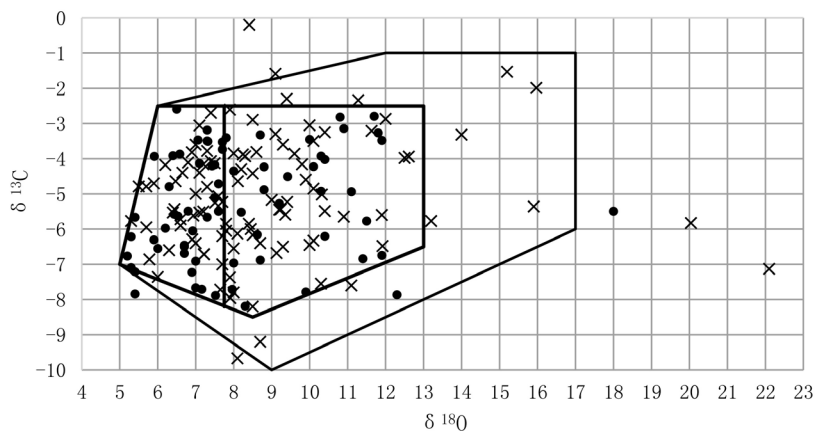


Figure 3. The starting points in occurrences with a linear trend (fat point, $n = 70$) and in other occurrences (oblique cross, $n = 103$). The outer contour PC-98%. The internal contour PC-90% includes 90% of points and is divided into two halves of PC-45%.

Subsequent statistical analysis of isotope data uses summary indicators characterizing carbonatite occurrences. Trend (linear regression) analysis was performed in 140 occurrences that satisfy two conditions: 1) there are three or more points; 2) the arithmetic difference between the maximum and minimum $\delta^{18}\text{O}$ values is more than 0.5‰. Trend lines under opposite conditions (less than three points and difference $\delta^{18}\text{O}$ less than 0.5‰) cannot be reliable. The linear regression equation $y = kx + b$ and the trend line are calculated in Microsoft Excel 97-2003. The complete database (it is too large to be here) contains a point diagram for each occurrence, a calculated angular coefficient k , a constant b , a coefficient of determination (approximation) R^2 .

Examples of point diagrams in order of increasing coefficient R^2 are shown in [Figure 4](#). According to the visual observation of the diagrams, the linear trend is absent or indistinct in the occurrences that have R^2 from 0.00 to 0.29. The number of such occurrences in the database is 70. The linear form of point fields begins to confidently be fixed from $R^2 \geq 0.30$ (occurrence 413. Chetlassky in [Figure 4](#)). The linear trend is found in 70 occurrences, where R^2 is from 0.30 to 0.99. The trend line is depicted as a vector directed upwards $\delta^{18}\text{O}$. Such a direction is taken in the literature on the geochemistry of carbonatites.

[Appendix](#) provides a summary Table with brief data on 173 carbonatite occurrences. The names of occurrences that are not in the database [8] are given without an ID number. Digital data include: 1) n , n^* is the number of paired values $\delta^{18}\text{O}-\delta^{13}\text{C}$ in occurrences without a linear trend (n) and with a linear trend (n^*); 2) middle point arithmetic average $\delta^{18}\text{O}-\delta^{13}\text{C}$ from among the values; 3) the starting point of the trend line or nonlinear field of $\delta^{18}\text{O}-\delta^{13}\text{C}$ points; 4) minimum initial ratio $^{87}\text{Sr}/^{86}\text{Sr}$. The position of carbonatite occurrences in the diagrams ([Figure 2](#) and [Figure 3](#)) can be determined using the table values.

Trend line and middle point for 70 occurrences in which a linear trend is revealed are shown in the diagram ([Figure 2](#)). Only the middle point is shown for the remaining 103 occurrences. The polygonal contour PC-98% is delineated. It includes about 98% of all middle points. The diagram shows that trend lines vary significantly in length. The horizontal span of the lines (the arithmetic difference $\delta^{18}\text{O}_{\text{max}} - \delta^{18}\text{O}_{\text{min}}$) ranges from 0.5‰ to 11‰, in 90% of cases it does not exceed 7.5‰, on average it is 3.5‰.

The slope of the trend line varies widely, as seen in [Figure 2](#). The slope is determined by the angular coefficient k . Statistical analysis of the coefficient is shown in [Figure 5](#). Three separate intervals of k are read on the point diagram: $-0.73 - 0.09$; $0.09 - 0.51$; $0.51 - 1.51$. On the rose diagram, the intervals are shown as sectors, and the average for the three sectors is shown as vectors. Sector k with a range of $0.09 - 0.51$ and a middle vector of 0.30 is sharply dominant. Sector $-0.73 - 0.09$ with a middle vector of -0.27 and sector $0.51 - 1.51$ with a middle vector of 0.96 have a subordinate meaning.

The averaged shape of the field of points for three groups of occurrences with a linear trend and for one group without a trend is modeled in [Figure 6](#). The

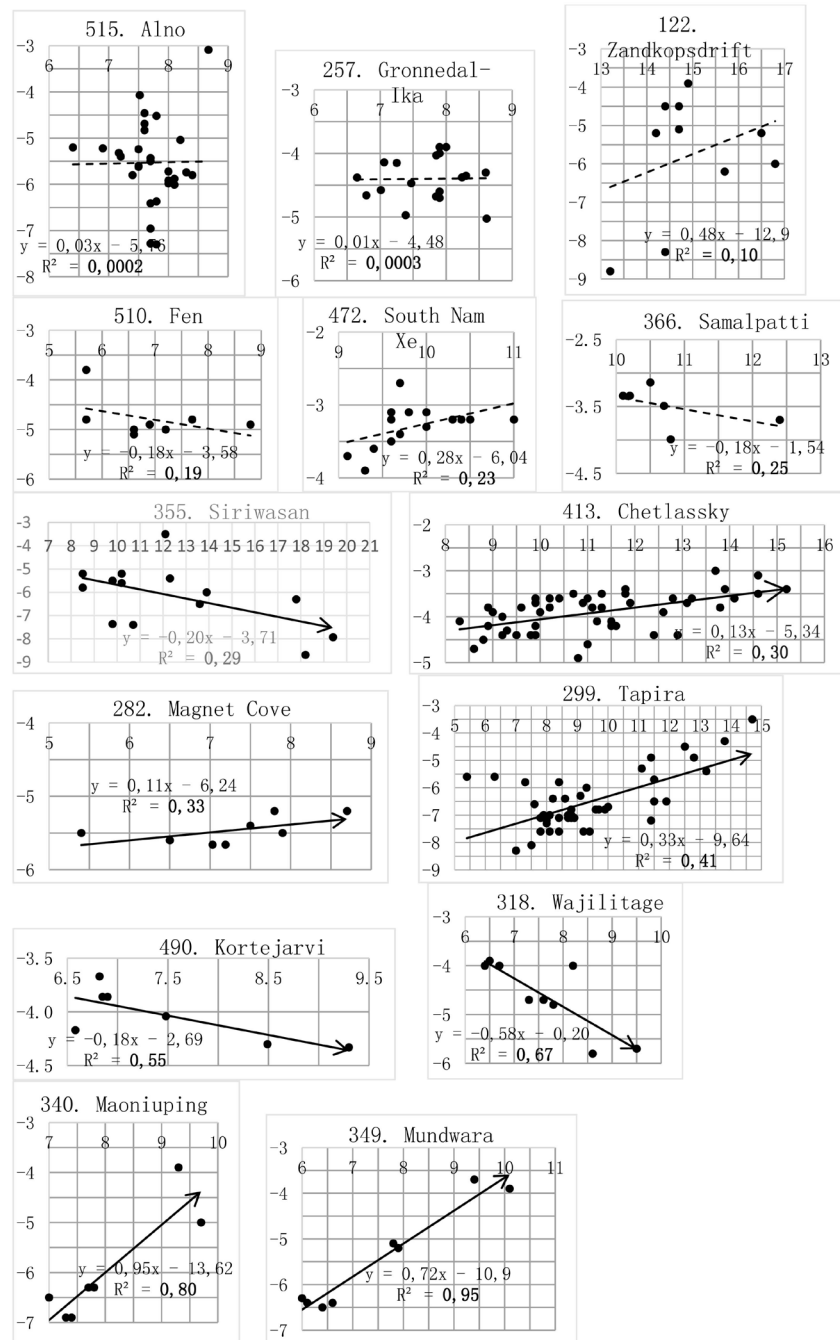


Figure 4. Examples of trend analysis of $\delta^{18}\text{O}$ (x-axis, ‰) and $\delta^{13}\text{C}$ (y-axis, ‰) values in carbonatite occurrences in order of increasing coefficient R^2 .

arithmetic average differences $\delta^{18}\text{O}_{\text{max}} - \delta^{18}\text{O}_{\text{min}}$ and $\delta^{13}\text{C}_{\text{max}} - \delta^{13}\text{C}_{\text{min}}$ are calculated in each group. Rectangles with sides equal to these averages are shown in **Figures 6(a)-(d)**. The modeled fields of points are inscribed in rectangles along the middle trend line. All fields in accordance with their averages are placed in **Figure 6(e)**. Comparison of the fields shows that the lack of a clear linear form in the field 6d is due to the increased variation in the $\delta^{13}\text{C}$ value. This may be due to the cumulative effect of trends 6a, 6b and 6c.

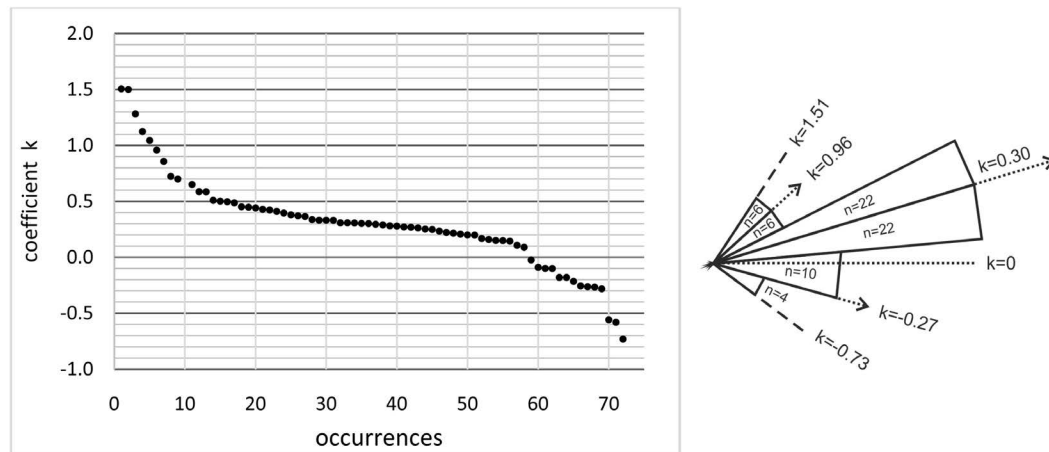


Figure 5. Point diagram (left) and rose diagram (right) of the angular coefficient k in the regression equation $y = kx + b$ in occurrences with the linear trend $\delta^{18}\text{O}-\delta^{13}\text{C}$. The point diagram shows separate intervals $k: -0.73 - 0.09$ (average -0.27); $0.09 - 0.51$ (average 0.30); $0.51 - 1.51$ (average 0.96).

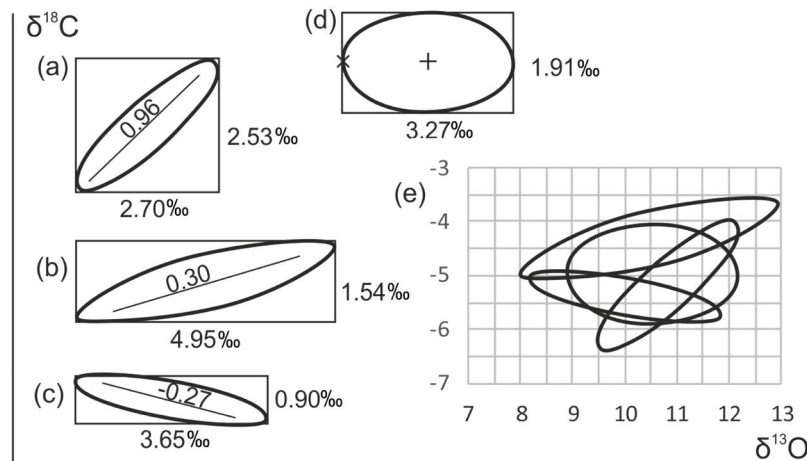


Figure 6. The averaged form of point fields: (a, b, c) occurrences with a linear trend with an angular coefficient of 0.96, 0.30 and -0.27 ; (d) occurrences without a linear trend with a middle point (straight cross) and a starting point (oblique cross); (e) comparison of the fields in the diagram.

Each carbonatite occurrence with a linear trend can be characterized by the starting point of the trend. The $\delta^{18}\text{O}$ of the starting point is equal to the minimum value in the statistical sample. The $\delta^{13}\text{C}$ value is calculated from the empirical regression equation. The values of $\delta^{18}\text{O}-\delta^{13}\text{C}$ starting points of the trends are given in the Table. Occurrences without a linear trend also imply the presence of a starting point. This follows from the previously made assumption that the nonlinear point field 6d in **Figure 6(d)** is the result of the cumulative influence of trends 6a, 6b and 6c. All trends are directed upwards $\delta^{18}\text{O}$, but in different directions along $\delta^{13}\text{C}$. Therefore, the starting point of field 6d must have $\delta^{18}\text{O}$ equal to the minimum of the statistical sample. The $\delta^{13}\text{C}$ value in some approximation can be taken equal to the average of the sample (**Figure 6(d)**). The $\delta^{18}\text{O}-\delta^{13}\text{C}$ of the starting point in the occurrences without the identified linear

trend is also given in the Table.

The diagram shows two groups of points (**Figure 3**): 1) the starting point of the trend line in the occurrences with a linear trend ($n = 70$); 2) the starting point of nonlinear fields in other occurrences ($n = 103$). The second group includes occurrences without a linear trend ($n = 70$), and also occurrences with only two points $\delta^{18}\text{O}$ - $\delta^{13}\text{C}$ ($n = 24$) and with a difference $\delta^{18}\text{O}_{\text{max}} - \delta^{18}\text{O}_{\text{min}} < 0.5$ ($n = 9$) that were excluded from the trend analysis. Visual analysis of the diagram allows to delineate the internal contour PC-90% in addition to the PC-98% contour justified in **Figure 2**. This contour includes a compact group of 90% starting points. The vertical line $\delta^{18}\text{O} = 7.9\text{\textperthousand}$ divides the contour PC-90% into two parts, each of which is 45% of the total number of starting points.

The contours of primary carbonatites PC-98%, PC-90% and PC-45% (left and right contours) are shown in the diagram (**Figure 7**). For comparison, the contours and points of primary igneous (mantle) carbonatites are given according to other authors. The closest is the left contour of PC-45% and the contour of Jones *et al.* [7]. The three middle vectors of the angular coefficient k are also shown in the diagram. The dominant trend $k = 0.30$ in the literature is usually associated with two factors that coincide in direction: 1) Rayleigh isotopic fractionation at high-temperature differentiation of carbonatite melts; 2) sedimentation (crustal) contamination of mantle melts. The second factor is illustrated by the directionality of the dominant trend on the contour of normal sedimentary rocks. The subordinate trend $k = -0.27$ is associated with the degassing of CO_2 from melts. Another subordinate trend $k = 0.96$ is not discussed in the literature. The beginning of the vectors is at the point (5‰ $\delta^{18}\text{O}$; -6.5‰ $\delta^{13}\text{C}$). The full sector of the angular coefficient (from -0.73 to 1.51) covers almost all occurrences from this point. Perhaps this point is close to the primary mantle source of carbonatites.

The used literature on O-C isotopy also contains data on the isotope composition of strontium. The minimum initial value of $^{87}\text{Sr}/^{86}\text{Sr}$ in 92 carbonatite occurrences is given in the Table. The field of minimum values in the coordinates $^{87}\text{Sr}/^{86}\text{Sr}$ - $\delta^{18}\text{O}$ is presented in the diagram (**Figure 8**). There is no correlation between the values. The oblique line in the diagram is the line of mixing the mantle source ($^{87}\text{Sr}/^{86}\text{Sr} = 0.702$; $\delta^{18}\text{O} = 5\text{\textperthousand}$) and the sedimentary contaminant ($^{87}\text{Sr}/^{86}\text{Sr} = 0.710$; $\delta^{18}\text{O} = 20\text{\textperthousand}$) at equal concentrations of strontium in the sources. The stable enrichment of carbonatites with strontium in comparison with sedimentary carbonates is known. Under this condition, a band of points above the mixing line may reflect crustal contamination of magmas. However, a wide scatter of points below the mixing line leaves room for other hypotheses, including contamination of the source in the mantle. The PC-98%, PC-90% and PC-45% contours, previously substantiated in the coordinates $\delta^{18}\text{O}$ - $\delta^{13}\text{C}$, are delineated in the diagram. The PC-45% contour is divided by the value $^{87}\text{Sr}/^{86}\text{Sr} = 0.704$ into two fields. The field $^{87}\text{Sr}/^{86}\text{Sr} < 0.704$ and $\delta^{18}\text{O} < 7.75\text{\textperthousand}$ can be considered as the primary mantle field in the O-C-Sr isotope system.

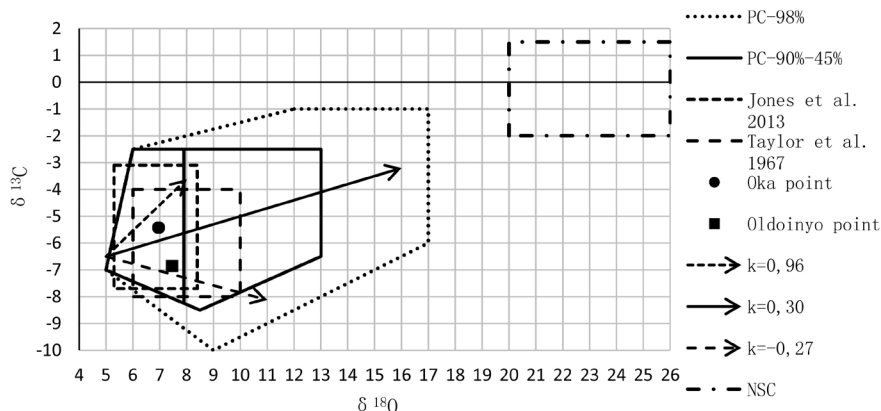


Figure 7. Fields and points of primary igneous carbonatites and middle trend vectors. NSC—normal sedimentary carbonates.

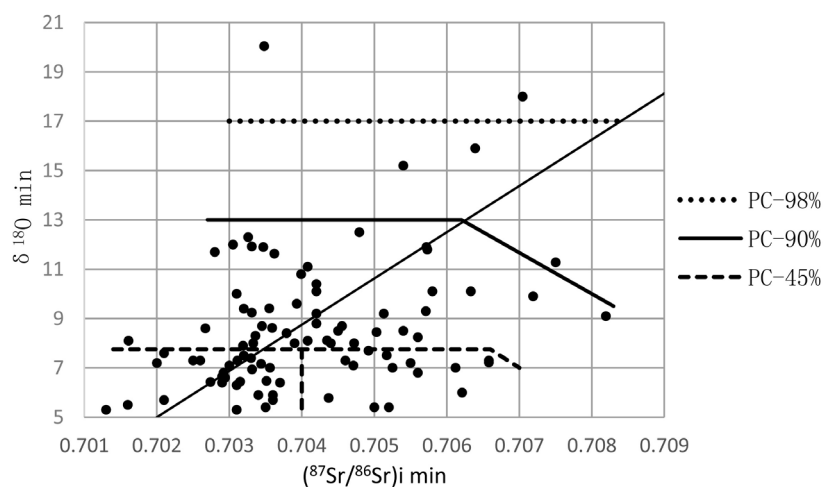


Figure 8. The isotope composition of strontium (minimum initial value) and oxygen (starting point) in carbonatite occurrences.

3. Conclusions

Data on the oxygen and carbon isotope composition of primary carbonatites for 173 carbonatite occurrences of the world were collected (1593 paired values of $\delta^{18}\text{O}$ - $\delta^{13}\text{C}$). Primary carbonatites are rocks without petrographic signs of secondary hydrothermal and exogenous mineral changes. Primary carbonatites demonstrate a wide variation of the $\delta^{18}\text{O}$ - $\delta^{13}\text{C}$ values and linear trends, which indicates the isotopic heterogeneity of carbonatite substance.

Linear regression analysis of $\delta^{18}\text{O}$ - $\delta^{13}\text{C}$ values reveals linear trends in half of the carbonatite occurrences. The trend with an average angular coefficient of 0.30 (positive correlation $\delta^{18}\text{O}$ - $\delta^{13}\text{C}$) sharply dominates. In the literature, this is explained by the Rayleigh high-temperature fractionation of carbonatite melts or by their sedimentary (crustal) contamination. The trend line span (arithmetic difference $\delta^{18}\text{O}_{\text{max}} - \delta^{18}\text{O}_{\text{min}}$) ranges from 0.5‰ to 11‰, on average it is 3.5‰. Increased trends (over 7.5‰) suggest the action not only of endogenous factors, but also the influence of secondary processes not recorded in petrographic ob-

servations.

The second trend with an average angular coefficient of -0.27 (negative correlation $\delta^{18}\text{O}$ - $\delta^{13}\text{C}$) is rarer. This trend is usually associated with the CO_2 degassing from melts. A rare third trend is not discussed in the literature. It has an average angular coefficient of 0.96 (positive correlation $\delta^{18}\text{O}$ - $\delta^{13}\text{C}$). The linear trend of $\delta^{18}\text{O}$ - $\delta^{13}\text{C}$ values is not detected in half of carbonatite occurrences due to increased variation of $\delta^{13}\text{C}$. This may be due to the combined action of different factors—contamination, high-temperature fractionation and degassing of melts.

The fields of primary carbonatites (PC) are delineated in the coordinates $\delta^{18}\text{O}$ - $\delta^{13}\text{C}$ (‰), including 98%, 90% and 45% of the numbers of occurrences. The PC-90% contour can be considered acceptable for primary carbonatites. In-depth petrographic and other argumentation of the primary nature of carbonates is required for occurrences outside this contour. The PC-45% ($\delta^{18}\text{O} < 7.75\text{\textperthousand}$) contour with a high probability includes only primary carbonatites with a mantle source of a carbonate substance and with minimal effect of isotope fractionation or contamination of melts. A greater influence of these factors is expected for occurrences in the PC-45% ($\delta^{18}\text{O} > 7.75\text{\textperthousand}$) contour.

Srontium in carbonatite occurrences has a wide variation of the initial $^{87}\text{Sr}/^{86}\text{Sr}$ ratio from 0.701 to 0.708 . This variation and the absence of correlation between $^{87}\text{Sr}/^{86}\text{Sr}$ and the $\delta^{18}\text{O}$ - $\delta^{13}\text{C}$ allow both mantle and crustal contamination of carbonatite magmas.

The stated statistical data on the O, C and Sr isotope composition in primary carbonatites leave room for additional and alternative judgments.

Conflicts of Interest

The author declares no conflicts of interest regarding the publication of this paper.

References

- [1] Deines, P. (1989) Stable Isotope Variations in Carbonatites. *Carbonatites: Genesis and Evolution*. Unwin Hyman, London, 301-359.
- [2] Demény, A., Sitnikova, M.A. and Karchevsky, P.I. (2004) Stable C and O Isotope Compositions of Carbonatite Complexes of the Kola Alkaline Province: Phoscorite-Carbonatite Relationships and Source Compositions. In: Wall, F. and Zaitsev, A.N., Eds., *Phoscorites and Carbonatites from Mantle to Mine*, Mineralogical Society Series 10, Mineralogical Society, London, 407-431.
<https://doi.org/10.1180/MSS.10.12>
- [3] Vladykin, N.V., Morikiyo, T., Miyazaki, T. and Tsypukova, S.S. (2004) Geochemistry of Carbon and Oxygen Isotopes of Siberian Carbonatites and Geodynamics. Deep Magmatism, Its Sources and Their Connection with Plume Processes, Irkutsk. 89-107. (In Russian)
- [4] Bell, K. and Simonetti, A. (2010) Source of Parental Melts to Carbonatites-Critical Isotopic Constraints. *Mineralogy and Petrology*, **98**, 77-89.
<https://doi.org/10.1007/s00710-009-0059-0>

- [5] Taylor, H.P., Frechen, J. and Degens, E.T. (1967) Oxygen and Carbon Isotope Studies of Carbonatites from the Laacher See District, West Germany and the Alnö District, Sweden. *Geochimica et Cosmochimica Acta*, **31**, 407-430.
[https://doi.org/10.1016/0016-7037\(67\)90051-8](https://doi.org/10.1016/0016-7037(67)90051-8)
- [6] Keller, I. and Hoefs, I. (1995) Stable Isotope Characteristics of Recent Natrocarbonatite from Oldoinyo Lengai. In: Bell, K. and Keller, J., Eds., *Carbonatite Volcanism: Oldoinyo Lengai and the Petrogenesis of Natrocarbonatites*, Proceedings in Volcanology, Vol. 4, Springer, Berlin, 113-123.
https://doi.org/10.1007/978-3-642-79182-6_9
- [7] Jones, A.P., Genge, M. and Carmody, L. (2013) Carbonate Melts and Carbonatites. *Reviews in Mineralogy & Geochemistry*, **75**, 289-322.
<https://doi.org/10.2138/rmg.2013.75.10>
- [8] Woolley, A.R. and Kjarsgaard, B.A. (2008) Carbonatite Occurrences of the World: Map and Database. Geological Survey of Canada, Ottawa.
<https://doi.org/10.4095/225115>

Appendix

Carbonatite occurrences: $\delta^{18}\text{O}$ - $\delta^{13}\text{C}$ values of middle and starting points of trends; minimum initial ratio $^{87}\text{Sr}/^{86}\text{Sr}$ (n^* – occurrences with a linear trend, n – other occurrences)

ID	Occurrence note	Country	Literary source	n, n*	Middle point		Starting point		
					$\delta^{18}\text{O}$	$\delta^{13}\text{C}$	$\delta^{18}\text{O}$	$\delta^{13}\text{C}$	$^{87}\text{Sr}/^{86}\text{Sr}$
1	2	3	4	5	6	7	8	9	10
1	InOuzzal	Algeria	Ouzegane <i>et al.</i> , 1988	7	9.38	-7.72	7.65	-7.72	-
5	Bailundo	Angola	Pineau <i>et al.</i> , 1973; Alberti <i>et al.</i> , 1999	8*	9.60	-5.34	6.70	-6.50	-
6	Monte Verde	Angola	Pineau <i>et al.</i> , 1973; Alberti <i>et al.</i> , 1999	15*	9.01	-4.53	5.30	-6.21	-
10	Tchivira-Bonga	Angola	Alberti <i>et al.</i> , 1999	7*	12.28	-3.74	9.42	-4.51	-
15	Lupongola	Angola	Alberti <i>et al.</i> , 1999	10*	9.23	-7.37	7.52	-7.88	-
16	Matongo	Bourundi	Dolenek <i>et al.</i> , 2015; Decree <i>et al.</i> , 2015	13*	7.54	-5.21	6.53	-5.63	-
19	Lueshe	Congo	Самойлов, 1984	2	7.90	-5.85	7.80	-5.85	-
21	Wadi Tarr	Egypt	Shimron, 1975	3*	6.43	-7.67	5.20	-6.76	-
29	Rangwa	Kenya	Suva <i>et al.</i> , 1975	5*	15.10	-5.56	10.10	-4.22	0.7042
33	Homa Mountain	Kenya	Dennis and Schrag, 2010	8*	8.51	-3.36	7.70	-3.52	-
34	Buru-siderite	Kenya	Onuonga, 1997	16	14.48	-3.94	12.61	-3.94	-
39	Kangankunde	Malawi	Dennis and Schrag, 2010; Nelson, 1987; Broom-Fendley <i>et al.</i> , 2017	9	8.49	-4.79	5.50	-4.79	0.7016
47	Chilwa Island	Malawi	Simonetti and Bell, 1994	16	11.48	-2.61	7.90	-2.61	0.7032
48	Tundulu	Malawi	Самойлов, 1984	2	12.35	-3.25	10.40	-3.25	-
51	Songwe Hill	Malawi	Broom-Fendley <i>et al.</i> , 2016	4*	11.13	-4.00	7.80	-3.40	-
64	Tamazert	Morocco	Bouabdellah <i>et al.</i> , 2010; Marks <i>et al.</i> , 2009	42	8.60	-5.62	6.94	-5.62	0.7033
73	Xiluvo	Mozambique	Melluso <i>et al.</i> , 2004	3*	9.63	-5.32	7.50	-5.10	0.7032
75	Swartbooisdrif	Namibia	Thompson <i>et al.</i> , 2002	2	8.01	-7.37	7.90	-7.37	-
78	Okorusu	Namibia	Le Roex and Lanyon, 1998	2	8.80	-4.64	8.11	-4.64	0.7043
79	Ondurakorume	Namibia	Le Roex and Lanyon, 1998	2	8.80	-4.64	6.47	-4.64	0.7035
82	Lofdal	Namibia	Vistorina Nandigolo, 2013	3*	8.08	-5.13	6.43	-5.57	0.7027
89	Dicker Willem	Namibia	Reid and Cooper, 1992	2	8.00	-5.00	7.00	-5.00	-
103	Phalaborwa	S. Africa	Suwa <i>et al.</i> , 1975	4	9.05	-3.85	8.00	-3.85	0.7039
105	Spitskop-calcite	S. Africa	Harmer, 1999; Suwa <i>et al.</i> , 1975	8*	14.14	-2.86	11.70	-2.80	0.7028
105	Spitskop-dolomite	S. Africa	Harmer, 1999; Suwa <i>et al.</i> , 1975	7	16.72	-1.99	15.97	-1.99	-
108	Nooitgedacht	S. Africa	Clarke, 1989	2	9.05	-4.30	8.20	-4.30	-
109	Kruidfonten	S. Africa	Clarke, 1989	5*	13.32	-2.40	10.90	-3.14	-
113	Premier Mine	S. Africa	Suwa <i>et al.</i> , 1975	4*	11.93	-6.50	11.40	-6.84	-
122	Zandkopsdrift	S. Africa	Ogungbuy <i>et al.</i> , 2015	10	14.95	-5.77	13.20	-5.77	-
126	Oldoinyo Lengai	Tanzania	Bell and Keller, 1995; Halama <i>et al.</i> , 2007	9	7.47	-6.86	5.78	-6.86	0.7044

Continued

127	Kerimasi	Tanzania	Zaitsev <i>et al.</i> , 2013	3*	9.43	-3.73	7.43	-4.20	-
142	Panda Hill (Mbeya)	Tanzania	Suwa <i>et al.</i> , 1975; Dennis and Schrag, 2010; Dolenek <i>et al.</i> , 2015	13	7.48	-4.70	5.90	-4.70	0.7034
155	Bukusu	Uganda	Самойлов, 1984	2	10.40	-2.90	8.50	-2.90	-
156	Tororo	Uganda	Nelson, 1987; Dennis, 2010	10*	9.03	-2.73	7.30	-3.49	0.7025
157	Sukulu	Uganda	Deines and Gold, 1973	8*	9.65	-2.66	7.30	-3.18	0.7026
173	Aley-calcite	Canada	Mader, 1986; Chakhmouradian <i>et al.</i> , 2015	6	8.53	-5.23	7.70	-5.23	-
176	Wicheeda-calcite	Canada	Trofanenko, 2014	2	6.94	-6.29	6.91	-6.29	-
176	Wicheeda-dolomite	Canada	Trofanenko, 2014	4	9.72	-5.59	9.36	-5.59	-
191	Eden Lake	Canada	Chakhmouradian <i>et al.</i> , 2008	9	8.08	-7.96	7.91	-7.96	-
196	Albany Forks	Canada	Suva <i>et al.</i> , 1975	9	10.30	-4.42	8.50	-4.42	-
229	St-Andre	Canada	Suva <i>et al.</i> , 1975	13*	10.78	-2.55	8.70	-3.32	-
230	Oka	Canada	Dennis and Schrag, 2010; Chen and Simonetti, 2015; Haynes <i>et al.</i> , 2003	26	6.96	-5.43	6.44	-5.43	0.7032
243	Aillik Bay-dolomite	Canada	Tappe <i>et al.</i> , 2006	3*	11.13	-2.77	10.80	-2.82	0.7040
243	Aillik Bay-dol-calc	Canada	Tappe <i>et al.</i> , 2006	11	10.75	-3.86	9.60	-3.86	0.7039
-	Paint Lake	Canada	Chakhmouradian <i>et al.</i> , 2010	2	8.45	-6.05	7.80	-6.05	-
-	Wekusko Lake	Canada	Chakhmouradian <i>et al.</i> , 2009	7	23.54	-5.83	20.04	-5.83	0.7035
249	Gardiner	Greenland	Nielsen and Buchardt, 1985	3*	10.97	-3.53	10.30	-3.93	-
253	Sarfartog	Greenland	Tappe <i>et al.</i> , 2011	2	12.02	-3.21	11.63	-3.21	0.7036
257	Grcnnedal-Ika	Greenland	Pearc 1997; Coulson <i>et al.</i> , 2003; Halama <i>et al.</i> , 2005	18	7.70	-4.40	6.65	-4.40	0.7029
258	Qaqarsuk-olivine sövite	Greenland	Knudsen and Buchardt, 1991	7*	7.47	-3.31	7.06	-3.47	-
258	Qaqarsuk-sövite	Greenland	Knudsen and Buchardt, 1991	4	7.28	-3.82	6.90	-3.82	-
258	Qaqarsuk-dolomite sövite	Greenland	Knudsen and Buchardt, 1991	5*	8.40	-3.29	7.32	-3.51	-
260	Igaliko	Greenland	Coulson <i>et al.</i> , 2003	9	13.02	-3.81	8.60	-3.81	0.7027
263	Bearpaw Mount.	USA	Dennis and Schrag, 2010	8*	8.70	-7.74	8.30	-8.19	-
265	Bear Lodge	USA	Moore, 2014	10	10.12	-9.20	8.70	-9.20	0.7046
272	Wet Mountains	USA	Armbrustmacher, 1979	4	8.88	-4.40	7.10	-4.40	-
275	Iron Hill	USA	Jones <i>et al.</i> , 2013; Hugh <i>et al.</i> , 1966	3*	8.33	-5.13	7.30	-5.66	0.7046
282	Magnet Cove	USA	Haynes <i>et al.</i> , 2003; Nelson <i>et al.</i> , 1988	8*	7.30	-5.50	5.40	-5.66	0.7035
285	Cerro Sapo	Bolivia	Schultz <i>et al.</i> , 2004	4*	9.84	-8.39	7.16	-7.71	0.7034
286	Chiaracke	Bolivia	Schultz <i>et al.</i> , 2004	3	12.10	-5.60	11.90	-5.60	0.7035
289	Angico dos Dias	Brazil	Antonini <i>et al.</i> , 2003	16	14.78	-6.48	11.92	-6.48	0.7033
293	Catalao II	Brazil	Vincenza Guarino <i>et al.</i> , 2016	10	8.79	-6.00	8.45	-6.00	0.7050
294	Catalao I	Brazil	P. F. de Oliveira Cordeiro <i>et al.</i> , 2011	5*	10.86	-5.74	9.20	-5.27	0.7051
296	Salitre	Brazil	Brod, 1999	12*	7.55	-6.90	6.90	-7.23	-
298	Araxa	Brazil	Santos and Clayton, 1995	4*	9.78	-6.98	8.70	-6.88	-

Continued

299	Tapira	Brazil	Brod, 1999 Gomide <i>et al.</i> , 2016;	45*	9.32	-6.54	5.40	-7.84	0.7052
303	Jacupiranga	Brazil	Comin-Chiaromonti <i>et al.</i> , 2007; Haynes <i>et al.</i> , 2003; Nelson, 1987	25*	7.28	-6.37	5.40	-7.21	0.7050
305	Barra do Itapirapua	Brazil	Andrade <i>et al.</i> , 1999 Santos and Clayton, 1995;	9*	8.34	-5.91	6.70	-6.46	-
306	Mato Preto	Brazil	Andrade <i>et al.</i> , 1999; Comin-Chiaromonti <i>et al.</i> , 2001	20*	12.35	-1.38	8.00	-6.96	0.7047
310	Chiriguelo	Paraguay	Censi <i>et al.</i> , 1989; Castorina <i>et al.</i> , 1997	20*	14.97	-6.36	9.90	-7.78	0.7072
318	Wajilitage	China	W. Song <i>et al.</i> , 2017	9*	7.62	-4.62	6.40	-3.91	0.7037
323	Bayan Obo-dike	China	Yang X <i>et al.</i> , 2000; Le Bas 2000	12*	14.24	-6.03	11.90	-6.75	-
-	South Qinling	China	C. Xu <i>et al.</i> , 2014	17*	11.45	-4.78	8.62	-6.16	0.7036
-	Qieganbulake	China	H.-M. Ye <i>et al.</i> , 2013	7	8.70	-3.88	8.24	-3.88	0.7056
332	Dashigou	China	C. Xu <i>et al.</i> , 2010	6	7.87	-6.71	7.22	-6.71	-
332	Yuantou	China	C. Xu <i>et al.</i> , 2010	2	9.16	-6.68	9.13	-6.68	-
337	Miaoya	China	Çimen <i>et al.</i> , 2018	10	11.14	-5.23	9.41	-5.23	0.7036
338	Shaxiongdong	China	C. Xu <i>et al.</i> , 2008	5*	7.58	-5.94	6.92	-6.05	-
340	Maoniuping	China	Z. Hou <i>et al.</i> , 2009	7*	8.03	-5.97	7.00	-6.91	0.7061
340	Muluozhai	China	Z. Hou <i>et al.</i> , 2009	5	8.70	-6.72	7.22	-6.72	0.7066
340	Lizhuang	China	Z. Hou <i>et al.</i> , 2009	2	11.00	-4.85	10.10	-4.85	0.7063
346	Sarnu-Dandali	India	Ray and Ramesh, 1999; Ray <i>et al.</i> , 2000	7*	8.91	-5.10	8.20	-5.52	-
349	Mundwara	India	Ray and Ramesh, 1999; Ray <i>et al.</i> , 2000	8*	7.54	-5.44	6.00	-6.55	-
350	Newania	India	Viladkar and Ramesh, 2014	7*	10.51	-4.24	7.60	-5.49	0.7021
355	Siriwasan	India	Viladkar and Gittins, 2016	14	12.50	-6.17	8.50	-6.17	0.7054
356	Amba Dongar	India	Gwalani <i>et al.</i> , 2010; Viladkar and Ramesh, 2014; Simonetti <i>et al.</i> , 1995	48	10.88	-4.16	7.20	-4.16	0.7055
356	Amba Dongar-dike	India	Viladkar and Ramesh, 2014; Gwalani <i>et al.</i> , 2010	21*	11.75	-4.11	7.60	-4.71	-
357	Swangkre	India	Ray <i>et al.</i> , 1999	7	9.51	-3.60	9.30	-3.60	-
358	Sung Valley	India	Ray <i>et al.</i> , 1999; Srivastava <i>et al.</i> , 2005; Viladkar and Ramesh, 2014	35	7.66	-3.06	7.10	-3.06	0.7047
360	Samchampi	India	Ray <i>et al.</i> , 1999	11	7.25	-3.60	7.00	-3.60	-
365	Hogenakkal	India	Pandit, 2002	4	8.23	-6.13	8.10	-6.13	0.7016
366	Samalpatti	India	Ackerman <i>et al.</i> , 2017	6	10.78	-3.50	10.10	-3.50	0.7058
367	Sevattur	India	Pandit, 2003; Kumar <i>et al.</i> , 1998; Ackerman <i>et al.</i> , 2017	12	8.93	-5.25	7.51	-5.25	0.7052
369	Mulakkadu	India	Pandit, 2002	5	7.44	-3.78	7.30	-3.78	0.7066
378	Matcha	Kirgystan	Vrublevskii, 2017	9*	20.73	-3.58	18.00	-5.49	0.7070
379	Hongcheon	S. Korea	Kim <i>et al.</i> , 2005; Kwon and Yeang, 2003	7*	9.53	-6.36	7.96	-7.71	-
-	Yonghwa	S. Korea	Jieun Seo <i>et al.</i> , 2016	7	9.23	-7.00	7.70	-7.00	-
380	Mushugai Khuduk	Mongolia	Владыкин и др., 2004	4	15.73	-1.53	15.20	-1.53	0.7054

Continued

383	Ulugei	Mongolta	Кулешов, 1986	12	9.94	-9.67	8.10	-9.67	0.7041
-	Zhlobin	Belarussia	Веретенников и др., 2007	4	22.73	-7.13	22.10	-7.13	-
393	Seblyavr	Russia	Кухаренко и Донцова, 1962	3	12.63	-6.33	10.10	-6.33	-
398	Khibiny	Russia	Zaitzev, 1996; Покровский, 2000	28*	9.23	-5.09	5.90	-6.30	0.7036
399	Ozernaya Varaka	Russia	Самойлов, 1984	2	12.90	-7.60	11.10	-7.60	-
400	Afrikanda	Russia	Самойлов, 1984	4	12.35	-7.55	10.30	-7.55	-
401	Lesnaya Varaka	Russia	Кухаренко и Донцова, 1962	2	11.85	-6.45	10.00	-6.45	-
405	Telyachi Island	Russia	Beard <i>et al.</i> , 1996	4*	9.12	-3.76	8.80	-4.23	-
406	Turiy Mys	Russia	Dunworth and Bell, 2001; Demeny <i>et al.</i> , 2004; Владыкин и др., 2004	17	7.94	-2.70	7.40	-2.70	0.7033
407	Kovdor	Russia	Плюснин и др., 1980; Владыкин и др., 2004	7	12.10	-2.30	9.40	-2.30	0.7032
408	Sallanlatvi	Russia	Demeny <i>et al.</i> , 2004	4*	14.63	-1.93	10.00	-3.45	-
409	Vuoriyarvi	Russia	Demeny <i>et al.</i> , 2004; Владыкин и др., 2004	15	8.09	-4.11	6.80	-4.11	0.7056
410	Tiksheozero	Russia	Щипцов, 1988	7	11.81	-5.65	10.90	-5.65	-
413	Chetlassky	Russia	Удоратина и др., 2014; Шумилова и др., 2012	54	11.01	-3.93	8.30	-3.93	0.7034
-	Dubravinsky	Russia	Луговая и др., 2012	13	10.98	-5.85	8.40	-5.85	-
414	Vishnevogorskyy	Russia	Nedosekova <i>et al.</i> , 2012, 2013	7*	7.53	-7.10	7.00	-7.67	0.7036
417	Guli	Russia	Владыкин и др., 2004	6*	8.45	-4.07	6.30	-4.79	0.7031
418	Odikhinchha	Russia	Плюснин и др., 1980	2	12.60	-6.40	10.00	-6.40	0.7031
420	Kugda	Russia	Покровский, 2000	2	9.9	-6.4	8.7	-6.4	0.7035
-	Potanino	Russia	Недосекова и др., 2012; Nedosekova <i>et al.</i> , 2013	8	8.16	-6.20	7.70	-6.20	-
-	Buldym	Russia	Недосекова и др., 2012; Nedosekova <i>et al.</i> , 2013	5	8.96	-7.80	8.00	-7.80	0.7044
426	Magan	Russia	Кравченко и Багдасаров, 1987	2	11.40	-4.60	9.90	-4.60	-
428	Essei	Russia	Кравченко и Багдасаров, 1987; Владыкин и др., 2004	9*	11.88	-3.27	8.00	-4.35	0.7033
-	East Taimyr	Russia	Proskurnin <i>et al.</i> , 2010	5	11.96	-4.18	6.20	-4.18	-
436	Up. Petropavlovka	Russia	Vrublevskii, 2015	10*	13.84	-2.64	11.80	-3.27	0.7057
437	Edelveis	Russia	Vrublevskii <i>et al.</i> , 2012	9*	13.81	-5.59	12.30	-7.86	0.7033
438	Tagna	Russia	Владыкин и др., 2004	3	12.30	-2.87	12.00	-2.87	0.7031
439	Nizhnesayansky	Russia	Doroshkevich <i>et al.</i> , 2016; Владыкин и др., 2004	13	6.95	-5.90	6.60	-5.90	0.7029
440	Verkhnesayansky	Russia	Владыкин и др., 2004	3*	7.10	-5.57	6.80	-5.49	0.7029
441	Kharly	Russia	Брублевский, 2003	12	16.62	-3.32	14.00	-3.32	-
443	Zhidoy	Russia	Morikiyo <i>et al.</i> , 2000	4	7.33	-5.53	7.10	-5.53	0.7030
-	Karasug-calcite	Russia	Nikiforov <i>et al.</i> , 2006	7*	11.56	-4.29	8.80	-4.88	0.7042
-	Karasug-siderite	Russia	Nikiforov <i>et al.</i> , 2006	11	11.44	-5.45	9.20	-5.45	0.7042
-	Karasug-Teli	Russia	Nikiforov <i>et al.</i> , 2006	8	11.25	-4.16	9.80	-4.16	-

Continued

-	Karasug-Ulatay	Russia	Nikiforov <i>et al.</i> , 2006	3*	11.70	-4.30	10.40	-4.02	-
445	Yuzhnoe	Russia	Никифоров и др., 2000; Рипп и др., 2000	4*	7.55	-5.60	6.20	-5.97	-
446	Khaluta	Russia	Никифоров и др., 2000; Рипп и др., 2000	8	12.03	-6.50	9.30	-6.50	0.7057
448	Oshurkovo	Russia	Никифоров и др., 2000; Рипп и др., 2000, 2014	10	10.74	-6.40	7.00	-6.40	0.7053
-	West.Baical-calcite	Russia	Savelyeva <i>et al.</i> , 2016	4	12.70	-3.98	12.50	-3.98	0.7048
-	West.Baical-dolomite	Russia	Savelyeva <i>et al.</i> , 2016	6*	12.37	-3.28	11.90	-3.48	0.7057
450	Veseloe	Russia	Doroshkevich <i>et al.</i> , 2007; Ласточкин, 2009	10	10.16	-1.59	9.10	-1.59	-
451	Pogranichnoe	Russia	Doroshkevich <i>et al.</i> , 2006	3	8.67	-0.20	8.41	-0.20	0.7038
452	Murun	Russia	Владыкин и др., 2004; Покровский, 2000	20	8.42	-7.36	6.0	-7.36	0.7062
453	Seligdar	Russia	Doroshkevich <i>et al.</i> , 2018	5	16.48	-5.36	15.90	-5.36	0.7064
458	Khani	Russia	Владыкин и др., 2004	2	8.55	-8.20	8.50	-8.20	0.7045
459	Ingili	Russia	Владыкин и др., 2004	2	8.05	-6.55	8.00	-6.55	-
460	Arbarastakh	Russia	Владыкин и др., 2004	3	8.27	-5.07	7.60	-5.07	-
462	Koksharovsky	Russia	Октябрьский и др., 2010	9	11.00	-5.17	9.00	-5.17	-
464	Eppawala	Sri Lanka	Manthilake <i>et al.</i> , 2008; Pitawala <i>et al.</i> , 2003	27*	14.27	-2.69	7.70	-3.73	0.7049
467	Karacayir	Turkey	Cooper <i>et al.</i> , 2011	2	11.39	-2.34	11.28	-2.34	0.7075
471	Chagatai	Uzbekistan	Шумилова и др., 2012; Лохов и др., 2007	11*	10.06	-1.71	6.50	-2.59	-
472	South Nam Xe	Vietnam	T. Nguyen Thi <i>et al.</i> , 2014	17	9.80	-3.30	9.10	-3.30	0.7082
476	Wallaby	Australia	Salier <i>et al.</i> , 2004	5	10.51	-5.44	9.24	-5.44	0.7033
477	Mt Weld	Australia	Nelson, 1987	2	8.05	-5.50	7.20	-5.50	0.7020
479	Yungul	Australia	Gwalani <i>et al.</i> , 2010	37*	13.84	-5.69	10.40	-6.20	-
481	Cummins Range	Australia	Downes <i>et al.</i> , 2014	6*	8.28	-4.10	7.50	-4.17	-
482	Mud Tank	Australia	Wilson, 1979	4	7.50	-4.13	7.50	-4.13	0.7032
484	Haast River-calcite	New Zealand	Cooper and Paterson, 2008	6*	8.97	-6.22	6.70	-6.69	-
484	Haast River-dolomite	New Zealand	Cooper and Paterson, 2008	4*	13.48	-5.18	11.50	-5.77	-
488	Sokli	Finland	Demeny <i>et al.</i> , 2004	7*	7.86	-3.76	7.10	-4.13	-
489	Laivajoki	Finland	Nykanen <i>et al.</i> , 1997	7*	6.81	-4.44	5.91	-3.93	-
490	Kortejärvi	Finland	Nykanen <i>et al.</i> , 1997	7*	7.49	-4.03	6.58	-3.87	-
492	Siilinjarvi	Finland	Nykanen <i>et al.</i> , 1997	6	9.22	-4.07	7.40	-4.07	-
497	Laacher See	Germany	Hugh <i>et al.</i> , 1966; Jones <i>et al.</i> , 2013	13	7.39	-6.60	6.30	-6.60	-
498	Rockeskyll	Germany	Riley <i>et al.</i> , 1999	3*	12.40	-5.07	11.10	-4.94	0.7041
499	Kaiserstuhl	Germany	Hubberten, 1988; Dolenek <i>et al.</i> , 2015; Dennis and Schrag, 2010	54	9.69	-5.95	5.70	-5.95	0.7036
-	Pelagonian Zone	Greece	Schenker <i>et al.</i> , 2018	6	10.75	-5.49	10.40	-5.49	0.7042

Continued

-	Mt. Vulture	Italy	Stoppa <i>et al.</i> , 2016; Rosatelli <i>et al.</i> , 2010	4*	10.90	-4.78	10.30	-4.93	-
510	Fen	Norway	Broom-Fendley <i>et al.</i> , 2016; Andersen, 1987	8	6.90	-4.79	5.70	-4.79	0.7021
515	Alnö	Sweden	Roopnarain, 2013; Hugh <i>et al.</i> , 1966; Jones <i>et al.</i> , 2013	29	7.71	-5.53	6.40	-5.53	0.7029
518	Chernigovsky	Ukraine	Луговая и др., 1978	11	8.49	-5.77	5.30	-5.77	0.7013
519	Loch Borralan	UK Scotland	Young <i>et al.</i> , 1994	2	10.36	-5.02	10.32	-5.02	-
520	Fuerteventura	Spain	Hoernle <i>et al.</i> , 2002; Шумилова и др., 2012	12	7.32	-5.72	6.60	-5.72	-
522	Sao Vicente	Cape Verdes	Hoernle <i>et al.</i> , 2002	2	7.85	-4.80	7.30	-4.80	0.7031
524	Fogo	Cape Verdes	Hoernle <i>et al.</i> , 2002	4*	6.58	-6.70	5.30	-7.09	0.7031